GROUND CONTROLLED PRECISION LANDING DELIVERY IN THE PRESENCE OF RADAR DISTURBANCES

Cort L. Durocher

MIT

DEPARTMENT OF AERONAUTICS & ASTRONAUTICS

FLIGHT TRANSPORTATION LABORATORY
Cambridge, Mass. 02139

R77-2

May 1977

GROUND CONTROLLED PRECISION LANDING DELIVERY IN THE PRESENCE OF RADAR DISTURBANCES

by

Cort Louis Durocher

Flight Transportation Laboratory
Massachusetts Institute of Technology
Cambridge, Massachusetts 02139

FTL Report R77-2
May 1977

Acknowledgement

The author would like to thank the following people whose continued support made this study possible. Special thanks go to Professor Robert W. Simpson for his advice and encouragement, and to Mark Connelly for his many hours of work keeping the simulator in operation. I would also like to thank the following people who assisted in system formulation:

Captain David Boyle
Professor Walter Hollister
Captain Thomas Jones
Dr. Wolf Kohn
Robert W. Mann, Jr.
Bruce Morgenstern
Captain Bud Vietor

TABLE OF CONTENTS

LIST OF FIGURES

List of Symbols

ALPSL	Wind shift angle at the top of the boundary layer
EPR	Exhaust pressure ratio
P	Power law parameter
PSIW	Heading of atmospheric wind
PSIWG	Heading of geostrophic wind
PSIWO	Heading of reference wind
RHO	Radar range to aircraft
RHOE	Radar range to aircraft with error
σ	Standard deviation
THETAE	Radar bearing to aircraft with error
THETAR	Radar bearing to aircraft
USTAR	Friction velocity at the surface
VG	Magnitude of geostrophic wind
VRGFA	Veering rate
VW	Magnitude of atmospheric wind
VWREF	Magnitude of reference wind
WS	Wind shear
X, Y	Aircraft coordinates
$\hat{X}$, $\hat{Y}$	Estimated aircraft coordinates
XR, YR	Radar coordinates
Z	Aircraft altitude
ZBL	Altitude of boundary layer
ZO	Roughness length
ZREF	Height of reference wind
ZSL	Altitude of surface layer

Chapter I

Introduction of Background Material

1.1 Introduction

The purpose of Air Traffic Control is to ensure separation of aircraft in the most efficient manner possible. The need for efficiency is becoming more important as air traffic continues to increase at a high rate. Terminal area traffic control is the area in which the greatest amount of effort is expended since this tends to be the limiting factor in airspace congestion.

The current Automated Radar Terminal System provides a monitoring function which was unheard of with previous systems. However, this is not sufficient in view of the increasing air traffic. More improvements are needed in the exchange of information between the ground controller and the aircraft. The proposed upgraded Air Traffic Control system will provide better data acquisition, communications service, and increased automation. Future systems should be capable of providing more complete automation in terms of command generation and delivery. These systems are called Strategic Navigation or Four-Dimensional Navigation.

The principle of these systems is to assign a route-time profile to each aircraft thus providing good management of energy, space, and runways. This method utilizes a fixed airspace structure with a variable flight path to de-randomize aircraft runway arrival time. The method favored by the Federal Aviation Administration consists of ground computation of heading, altitude, and airspeed commands which

are broadcast to the aircraft via digital data-link. These commands can be either visually displayed for manual operation by the pilot or at some future time directly tied into the aircraft auto-pilot.

The purpose of this study is to simulate the flight of an aircraft on a terminal approach in a Four-Dimensional Navigation environment using discrete control commands. During the flight, position information is estimated from noisy radar observations. Speed is estimated from these observations and is used in a timed delivery algorithm to determine when to issue commands to the aircraft. Time control precision will be experimentally determined in the presence of the radar disturbance and accuracy of the Four-Dimensional Navigation task in the presence of this uncertainty will be quantified.

A number of studies have previously been conducted to determine fix-to-fix and runway arrival time accuracy. These studies neglected the effect of wind and assumed perfect radar position information. For this reason a comprehensive model for these two effects was developed.

1.2 Wind Model and Simulation

A wind model was developed and programmed based on a proposal made by Malherbe [1]. This wind model divided the atmosphere into three regions. The surface layer extended from the surface to an altitude of three hundred feet. The boundary layer height was dependent upon wind magnitude and extended up to about two thousand feet for moderate wind conditions. The free atmosphere was that space above the boundary layer and below ten thousand feet.

The altitudes encountered in this simulation are from two to six thousand feet so that the entire flight is performed in the free atmosphere. The wind in this region is a mean wind with wind magnitude and direction a function of altitude and surface wind. Wind shear and veering rate are assumed constant and provide variable magnitude and direction for a free atmospheric wind.

Several parameters must be specified to compute the free atmospheric wind. Wind shear, veering rate, and surface roughness must be known. A value of .007 seconds^{-1} was chosen for wind shear. This provides a smooth profile with altitude. In the northern hemisphere, southerly winds veer (shift clockwise) while northerly winds back (shift counterclockwise). A veering rate of .7 degree/100 feet was chosen. The roughness parameter describes the ground surface and was chosen as .15 foot. This value is recommended for airports by the British Air Registration Board.

Wind computation starts with the determination of the absolute height of the boundary layer and then computes the wind at that altitude (geostrophic wind). An approximation for boundary layer height is:

$$ZBL = \frac{246\ VWREF}{\sin \phi \log\left(\frac{ZO + ZREF}{ZO}\right)}$$

where ϕ is the latitude of the airport (42°N for Boston).

In the boundary layer the wind magnitude obeys the power law so

the geostrophic wind magnitude is:

$$VG = VWREF \left(\frac{ZBL}{ZREF} \right)^{P}$$

The value for P varies with the roughness of the ground and was chosen as one tenth for this simulation.

The shift angle of the wind at the top of the boundary layer can be approximated by:

$$\sin(ALPSL) = 10.7 \frac{USTAR}{VG} \left(\frac{ZREF - ZSL}{ZBL} - 1 \right)$$

where:

$$USTAR = \frac{.35\ VWREF}{\ln\left(\frac{ZO + ZREF}{ZO} \right)}$$

With these calculations completed, the geostrophic wind is known. It has a magnitude equal to VG and a direction equal to:

$$PSIWG = PSIWO - ALPSL$$

The free atmospheric wind is then calculated from the following relationships:

$$VW = VG + WS(Z - ZBL)$$

$$PSIW = PSIWG + VRGFA \left(1 - \frac{|PSIWO|}{90} \right) (Z - ZBL)$$

The wind profile used for altitudes from two to six thousand feet is displayed in Figure 1.1.

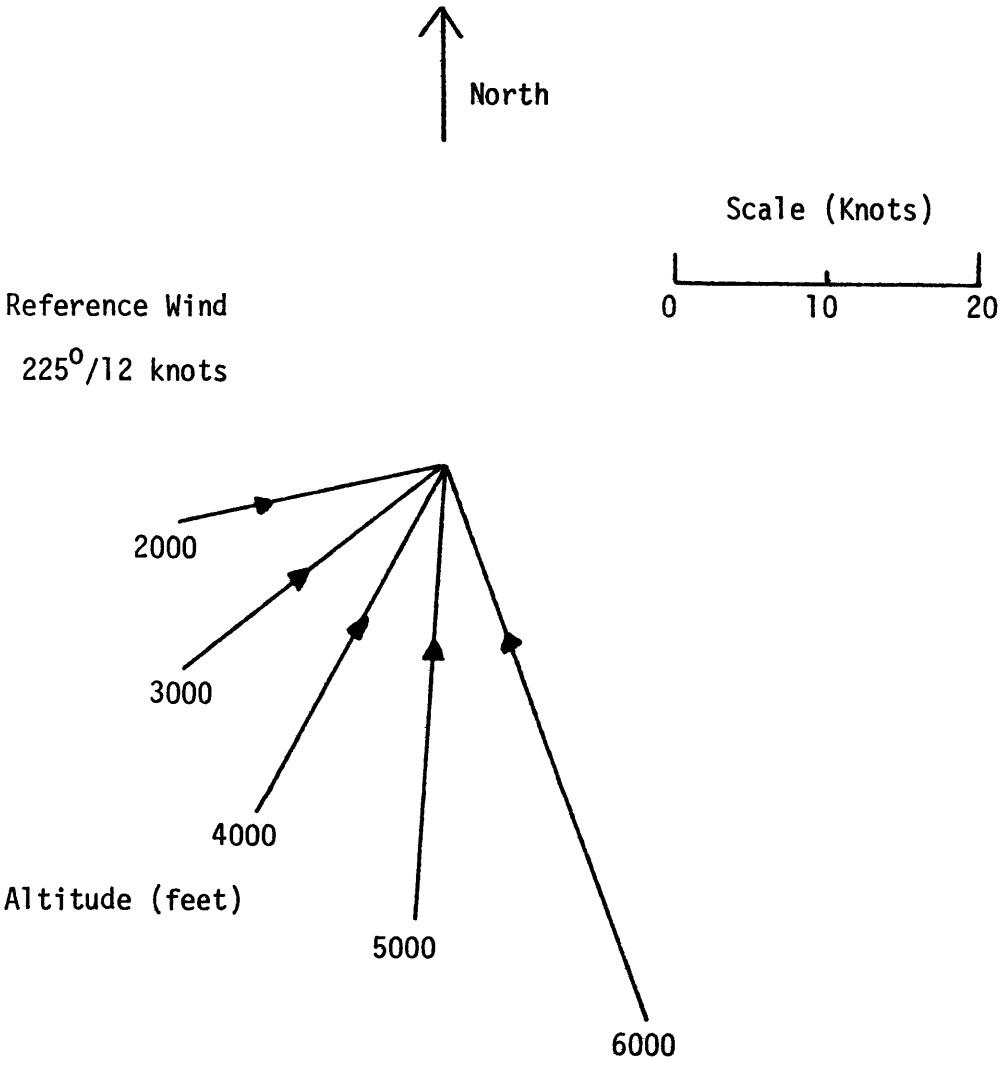

Figure 1.1 Wind Profile

1.3 Radar Model and Simulation

All radar yields only noisy information. Radar position error is a function of performance for any particular piece of radar equipment. This position error is characterized by standard deviations in range and bearing for each observation of the radar set. These standard deviations give an approximate aircraft position. This noisy position information is used by the ground based computer to determine when to issue time delivery commands.

The radar model used was similar to one developed by Malherbe [1] and reproduced radar noise by assuming the noise to be Gaussian white noise, independent of the distance from the radar. A block diagram of the radar model is shown in Figure 1.2.

The radar model used a random number generator to determine aircraft position after standard deviations in range and bearing were known. A multiplicative process [2] was used since it provided random numbers using very little computation time. This process generated twenty uniformly distributed numbers and then summed, averaged, and biased them to provide a Gaussian distribution with a mean value of zero.

The radar model could accommodate any standard deviation in bearing and range. The model could also accept different radar site positions. For the simulation, the radar was fixed at a location close to the runway.

Three different radar systems were tested along with the no error case. The least accurate radar tested was the current airport surveil-

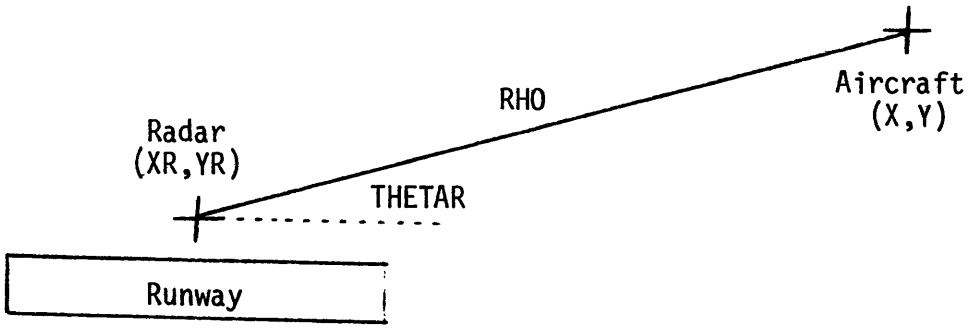

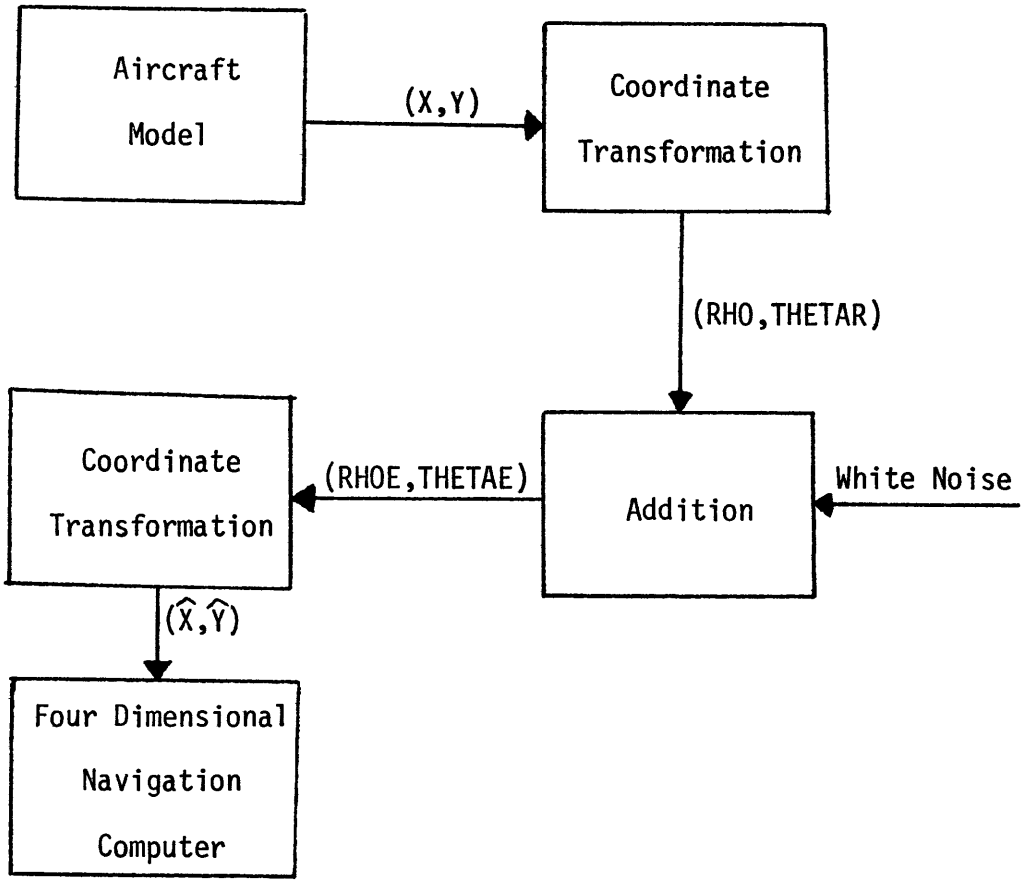

Figure 1.2 Radar Model

lance radar. This radar has an error with standard deviations in range and bearing equal to 250 feet and .25 degrees [3]. The performance of the next radar was characterized by standard deviations of 110 feet and .14 degrees. This performance is theorized for current radar equipment with an improved digital quantizer added to the radar processing equipment. The third radar performance is that of the Discrete Address Beacon System currently being tested. Personnel at Lincoln Laboratory supplied test results of 30 feet and .035 degrees for standard deviations of error. A no error case was included to provide a base line for comparison.

Groundspeed errors for lateral tracking from a radar site are shown in Figure 1.3 for the different radars modeled. These errors are the result of taking the difference between the radar position for two consecutive radar pulses. The pulse interval was four seconds.

1.4 Simulation Facility

The aircraft simulation facility consists of an Adage AGT-30 digital computer, a fixed base cockpit simulator, and associated hardware. The cockpit was built from a Boeing supersonic transport preprototype. The instrumentation, switches, and interior panels are representative of a Boeing 707. The Adage computer simulates the aircraft dynamics, performs all necessary command calculations, and generates the flight instruments on a cathode ray tube using a vector generator. The Adage has a two microsecond cycle time and sixteen thousand bits of memory and is equipped with dual disk drives. The

Radar Case	Error Standard Deviation		Groundspeed Error
	Range	Bearing	
0	0	0	0
1	30'	.035°	8 knots
2	110'	.14°	28 knots
3	250'	.25°	51 knots

Figure 1.3 Groundspeed Error

cockpit, computer, and associated hardware are shown in Figure 1.4.

1.5 Approach Geometry

The approach geometry for a Four-Dimensional Navigation scheme must provide flexibility in the time domain and be consistent with enroute and terrain limitations in the area of the airport. For this reason a single delay fan approach was developed and tested. This delay fan allows for a maximum delay of five minutes using both path and speed controls. The nominal flight path is in the center of the delay fan so the arrival time can be shifted plus or minus 150 seconds. The overall system geometry is shown in Figure 1.5.

For the purposes of the testing a single aircraft was used with the right hand delay fan. This geometry is shown in Figure 1.6 with the location of the timed delivery commands given. A detailed explanation of these commands is included in section 1.7. In a multiple aircraft case, aircraft would be assigned a left or right pattern dependent upon their arrival heading and time. Separation can thus be accomplished by time, altitude, and pattern. The limiting case as far as aircraft proximity occurs when one aircraft is at the final approach fix. The minimum mileage separation for 60 second time interval arrival is 2.9 miles, and for 72 second time interval is 3.65 miles. Final approach speeds were always 160 knots.

The complete approach is broken up into two segments. The first segment is the timed delivery algorithm which is the subject of this study. The second segment guides the aircraft from the final approach

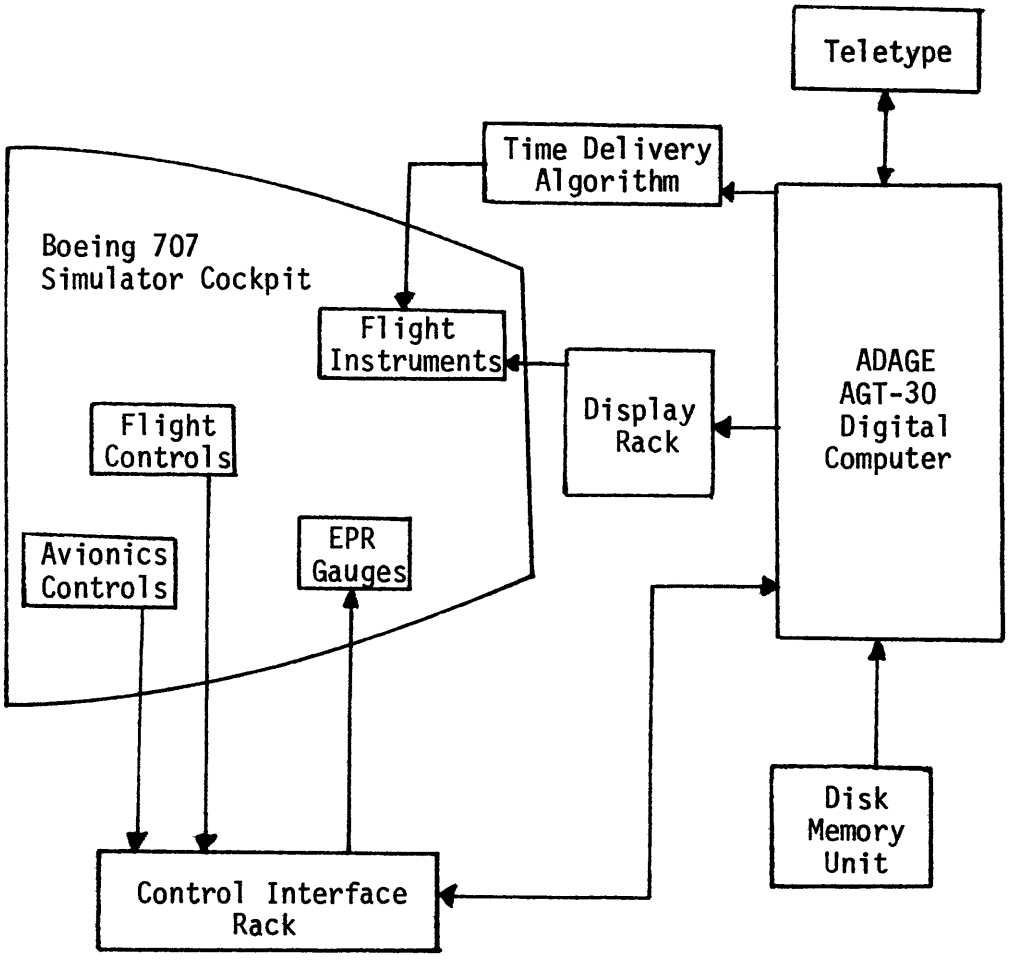

Figure 1.4 Simulation Facility Block Diagram

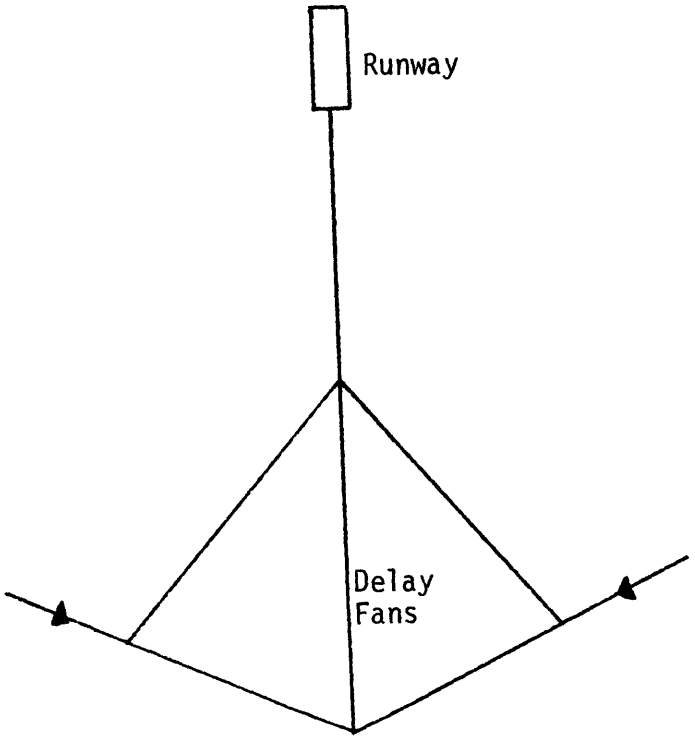

Figure 1.5 System Geometry

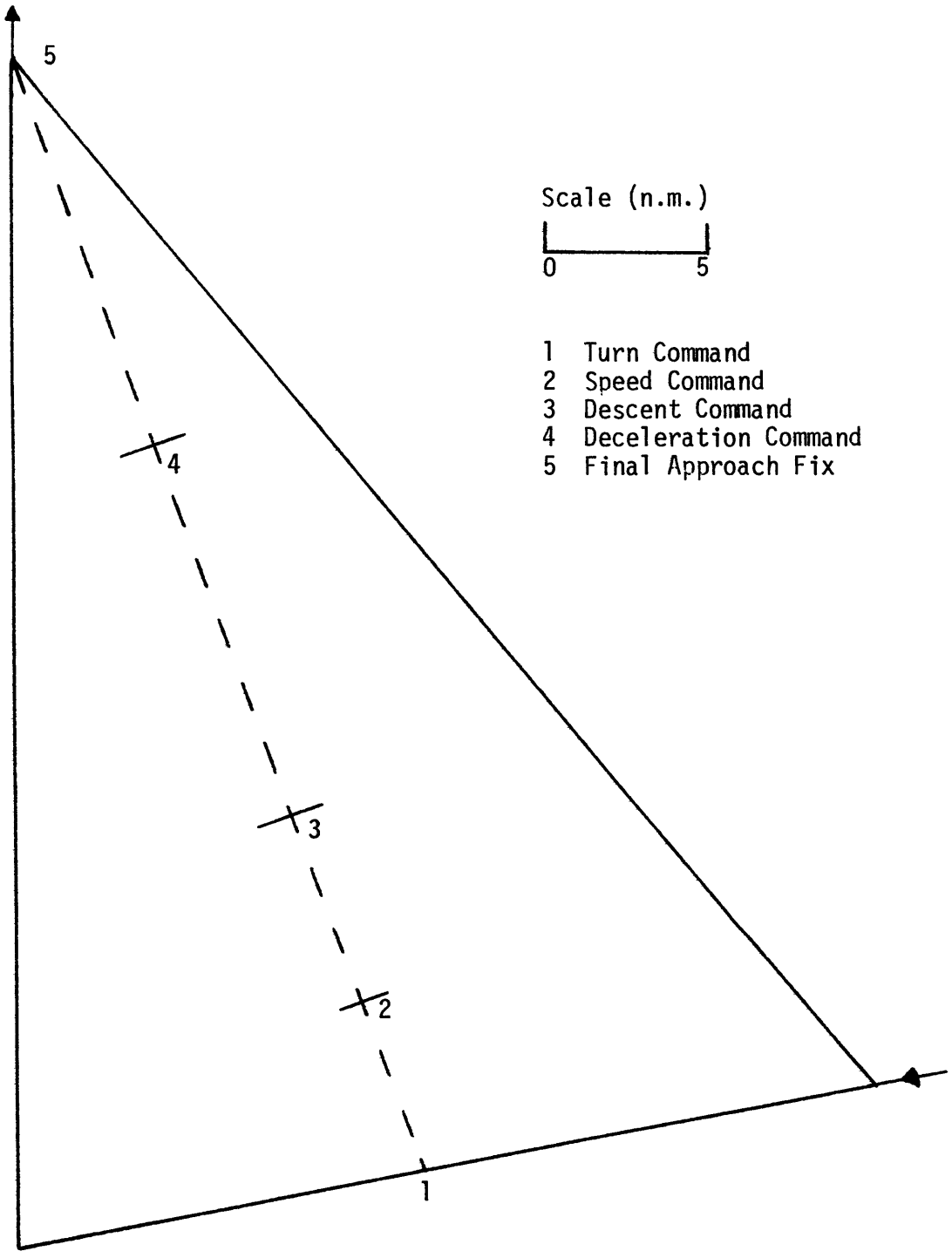

Figure 1.6 Delay Fan Geometry

fix to the runway. This segment could be a continuation of the first as in previous studies or could make use of a new idea developed by Hsin [4] called path stretching. This method is a formulated optimal control problem which will be discussed in section 1.6. Typical trajectories are shown in Figure 1.7. In this case the timed delivery algorithm delivers the aircraft to the final approach fix in a time window and the path stretching maneuver delivers the aircraft to the runway at the optimum time. This method provides a great deal of flexibility during the final phase of the approach.

1.6 Optimal Path Stretching

The final approach problem can be broken down into two phases. The first of these is the approach delivery problem. This problem is solved with a timed delivery algorithm in the approach metering zone. Optimal path stretching solves the second phase, the precision delivery problem in the precision delivery zone. These areas are displayed in Figure 1.8. When the aircraft is in the approach metering zone, the primary consideration is on spacing requirements between aircraft. When the aircraft is in the precision delivery zone, the emphasis is on the final delivery time.

Hsin [4] developed a minimum effort path stretching routine using the Newton-Raphson method which could be solved in real time on a computer. This method utilized a constant speed approach minimizing control effort to arrive at the runway at a designated time. This is a typical two point boundary value problem with initial and final

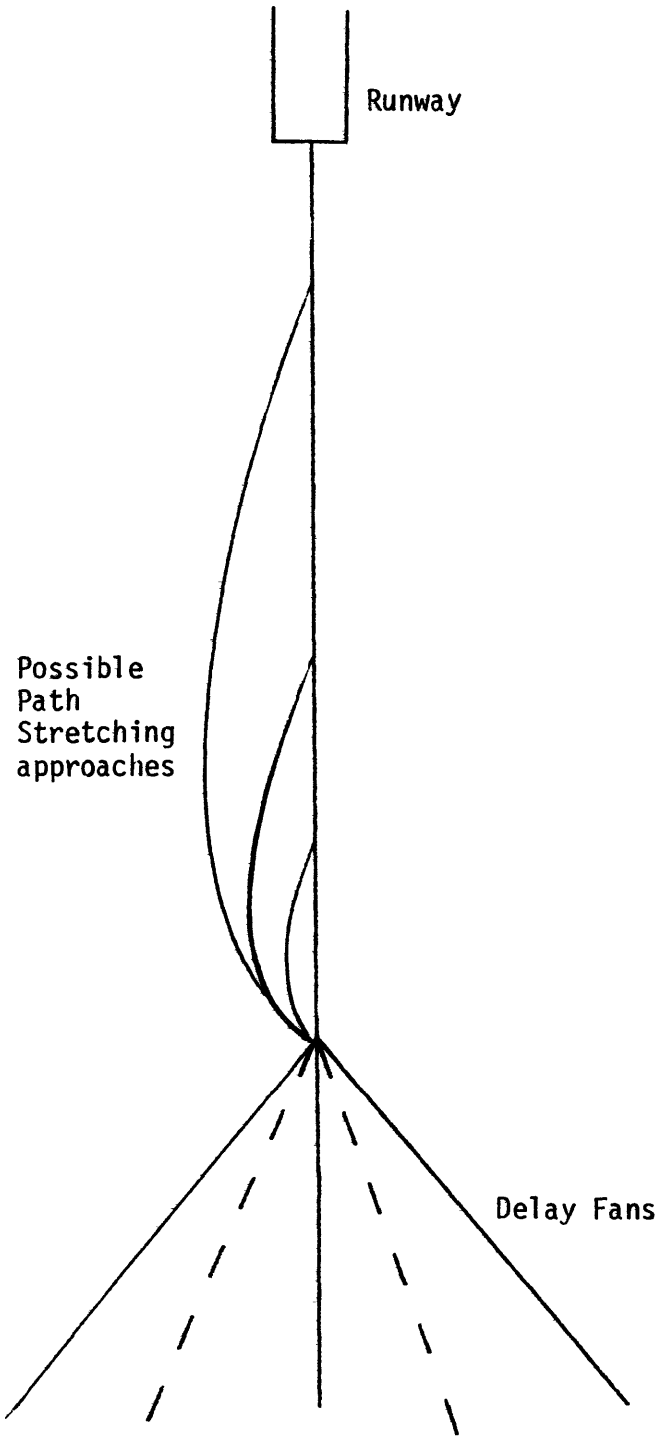

Figure 1.7 Path Stretching Geometry

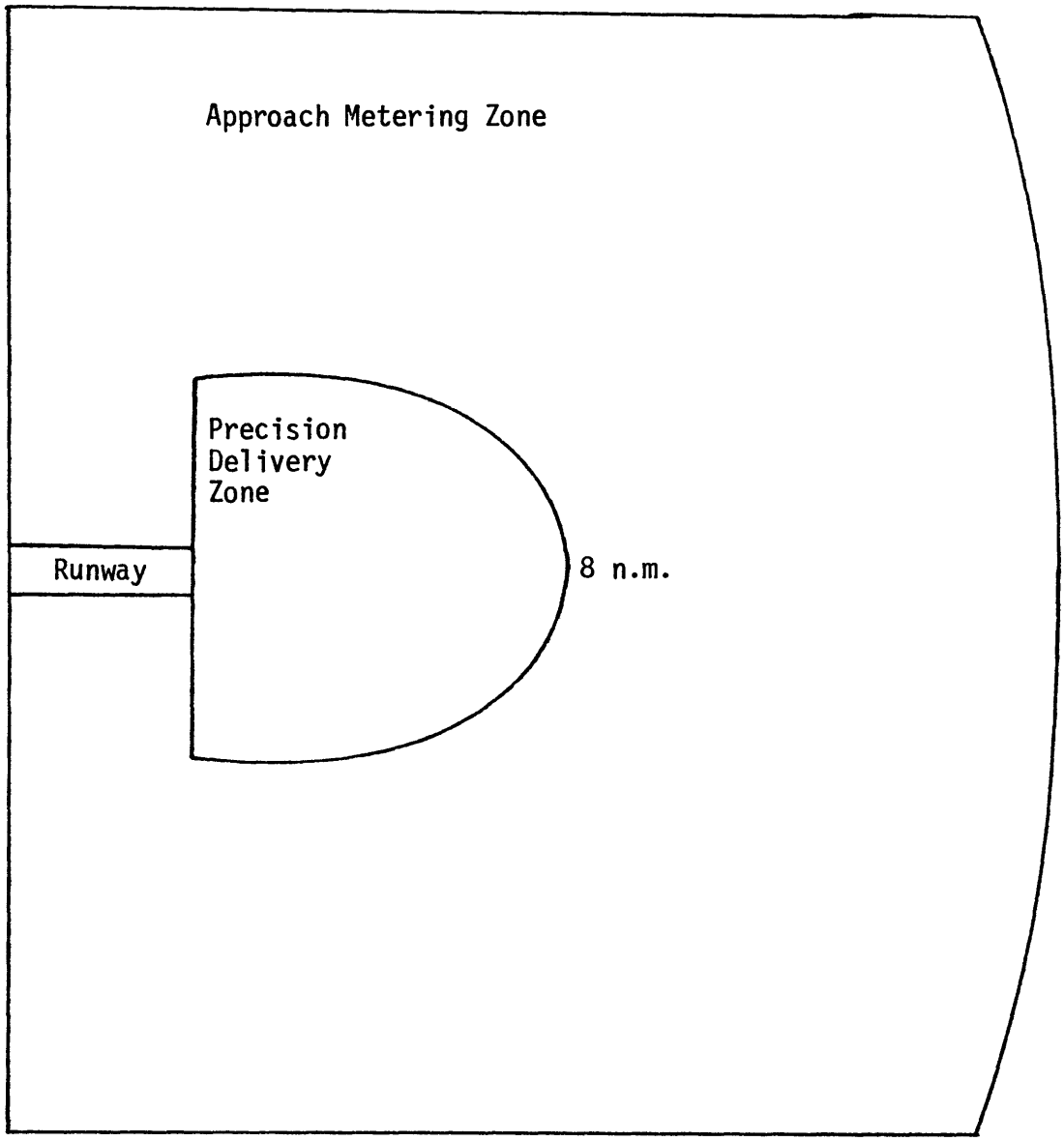

Figure 1.8 Zonal Geometry of Terminal Areas

conditions specified and a fixed terminal time. This automated minimum effort path stretching routine, given initial conditions and required delivery time, can generate a nominal horizontal flight path in a few seconds. The output can be a heading and speed command or a turning rate command. This is sent to the flight command generator for issuance to the pilot or autopilot. It is theorized that a simple routine of this type be applied to the aircraft delivery problem after arrival in the precision delivery zone.

1.7 Implementing Delivery Commands

The Four-Dimensional Navigation profile includes four computer generated commands. This algorithm was developed by Morgenstern [5] with major revision by the author. The aircraft simulation starts five nautical miles from the delay fan at 6000 feet and 220 knots indicated airspeed. The nominal arrival time at the final approach fix is 486 seconds.

In order to issue a turn command at the proper point, the computer uses runtime, present aircraft position, and a forecast wind. The turn command is issued at a point that will allow a standard rate turn to the commanded course followed by an indicated airspeed of 220 knots while tracking inbound.

Fifty seconds later, a speed command is sent to the aircraft. This speed will be very close to 220 knots. The difference between the commanded airspeed and 220 will be the correction needed for any deviation from a standard rate turn performed by the pilot and any inaccuracies in bearing from the radar. Since the aircraft is about

20 miles from the radar facility at this time, and tracking transverse to the radar site, a small error in bearing can advance or delay the turn command. For this reason, a fine tuning airspeed command is needed immediately after the turn is completed.

The descent command is issued at a fixed time. The descent phase allows for five seconds of pilot delay time after the command is issued, a 2000 feet per minute rate of descent, and five seconds to level-off at 2000 feet.

After the level-off is completed at 2000 feet the range to the final approach fix and time remaining are computed every four seconds to determine when to issue the deceleration command. The deceleration phase includes a deceleration rate of two knots per second. The commanded airspeed during this phase is decreasing at this rate. At the conclusion of the deceleration, the aircraft flies at 160 knots to the final approach fix. Closed loop speed control was implemented during this phase of the approach but was later abandoned as unnecessary.

During the entire approach, the wind is compensated with the commands. A forecast wind is used for the turn and airspeed commands. Actual along-course wind is used for the deceleration command. The complete simulation block diagram is depicted in Figure 1.9.

Commands are transmitted to the aircraft via digital data-link. During the simulation, commands are displayed in a small window below the attitude indicator. The pilot received course, altitude, and airspeed information. The commands were presented in a four character

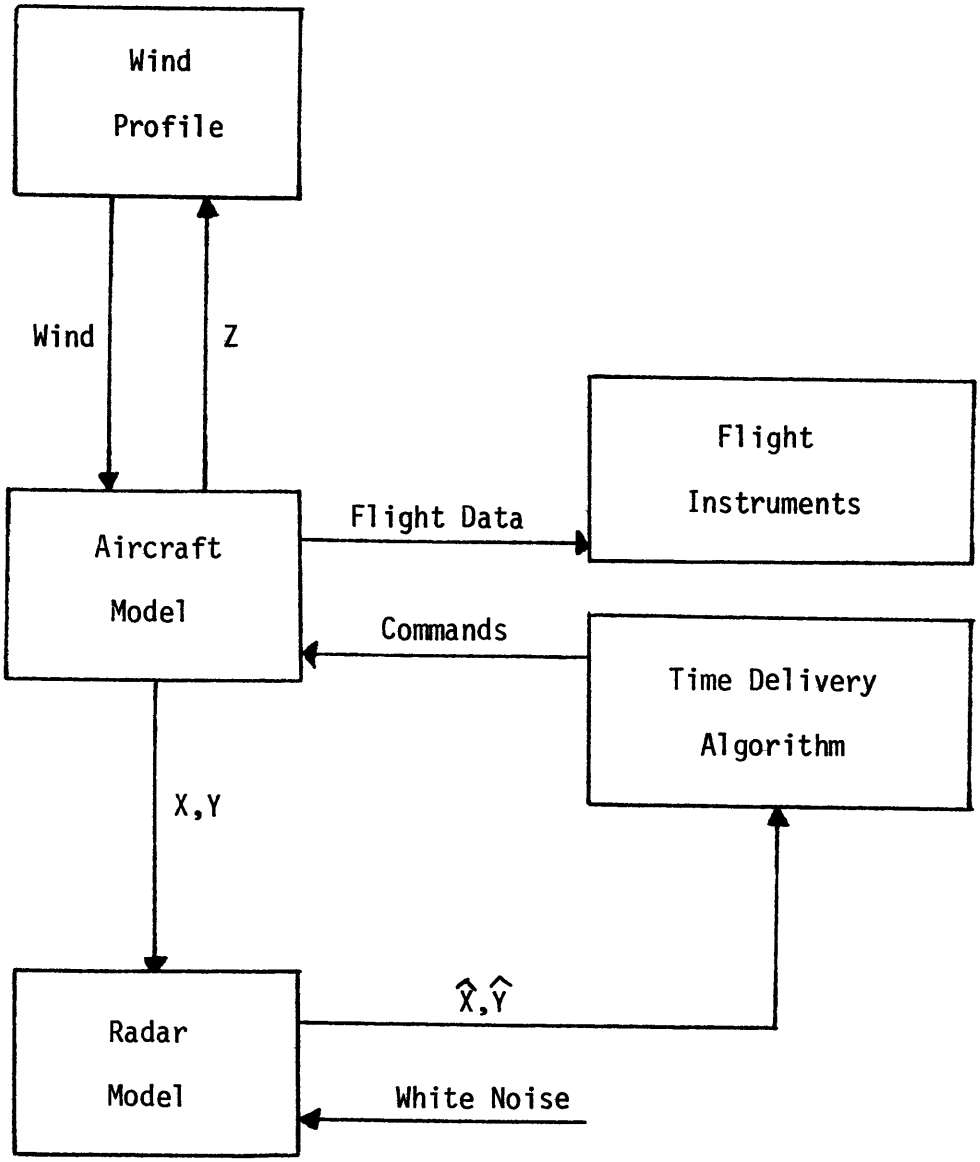

Figure 1.9 Simulation Block Diagram

message format:

C190 (Course-190 degrees)

S220 (Speed-220 knots)

A020 (Altitude-2000 feet)

All commands flash until acknowledged by the pilot with a switch located on the control wheel. Triangular shaped command bugs on the airspeed indicator, altimeter, vertical velocity indicator, and horizontal situation indicator display all command information.

Chapter II

Experimentation and Results

2.1 Introduction

The objective of the experimentation phase was to evaluate the system geometry and concept described in Chapter One. To accomplish this objective, eight subject pilots were recruited to fly the simulation. A summary of pilot experience and flight hours in included in section 2.2. These subject pilots were also asked to evaluate the simulation facility. The response is included in section 2.3.

The experimentation took on three distinct phases. Although the geometry and the overall conduct of flying the terminal approaches were unchanged, the method of delivery was altered to find the most accurate system consistent with pilot workload.

The first phase of testing included a closed loop speed control during the last sixty seconds prior to arrival at the final approach fix. It was postulated that this would provide last minute corrections and would improve delivery accuracy. Although the deceleration command was issued at a variable time, it took into effect a fixed rate of deceleration. It was thought that this deceleration would cause errors since rates are more difficult to maintain than fixed parameters. The programmed rate of descent was two knots per second and this schedule was displayed on the airspeed indicator with a moving airspeed bug.

Once the deceleration to 160 knots was completed, the computer would compute a wind corrected airspeed every four seconds based on

estimated aircraft position. The result would be displayed on the airspeed indicator with the airspeed bug. Airspeed limits during this phase were 130 and 220 knots. The stall speed of the aircraft was about 106 knots and a safety margin was added to prevent flying very close to a stall. Also, the aircraft power response is in a region of reversed operation at this low airspeed. This means that it takes more power to fly slower. Because of this fact the workload at low speed is considerably higher and detracts from pilot attention to course and altitude limitations. The 220 knot limitation was a structural one as this speed produces the maximum permissible amount of dynamic pressure on the flaps. Because of these imposed limitations, it was possible for a pilot to get himself into a situation where he did not know exactly how late or early his arrival time would be.

The commanded airspeed displayed on the airspeed indicator would correct to an on time arrival at the final approach fix. For the zero radar error case, estimated and actual aircraft position were the same, and the commanded airspeed would be stable if actual and commanded airspeed were the same. If the actual airspeed were higher than commanded, the next computation would correct for this and display a lower commanded airspeed.

With a radar error, the display was quite different. Since the radar errors were Gaussian, the commanded airspeed bug would be at a different airspeed after each computation. No smoothing algorithm was employed. The subject pilots were briefed on this and told to smooth these commands themselves. The difference between two successive

commanded airspeeds increased with an increase in radar error. Closed loop speed control was terminated when the aircraft reached a position within a half mile from the final approach fix. The results of these tests are discussed in section 2.4.

Phase two and three testing precipitated from the results of the phase one tests. The configuration changes and results will be discussed in sections 2.5 and 2.6.

2.2 Pilot Experience

The pilots recruited for the experimentation were from the M.I.T. community or commercial airlines servicing the Boston area. The summary of subject flight hours and subject experience is included in Figures 2.1 and 2.2.

With one exception, the pilots were very experienced. One general aviation pilot was tested to determine if the terminal approach information was displayed in a manner easily interpreted by novice instrument pilots. The results were satisfactory.

Two of the pilots had flown earlier Four-Dimensional Navigation simulations and four had flown the M.I.T. simulator before. Of the eight subjects, two were commercial airline pilots and five were military high performance jet pilots. Five pilots had flown multiengine jets and two pilots had flown aircraft similar to the Boeing 707.

In addition, three of the subjects were essentially non-current. They had little or no flying time in the previous twelve months as their present jobs did not require active flying. Only three of the

Subject Number	Flight Hours	Instrument Hours	Simulator Hours	Hours Last 12 Months
1	1500	200	200	200
2	3500	800	100	100
3	5500	1000	100	15
4	1955	400	150	0
5	388	65	5	50
6	25000	500	400	700
7	2050	200	100	20
8	8000	2000	100	500

Figure 2.1 Subject Flight Hours

Subject Number	Aeronautical Ratings	Types of Aircraft Flown
1	Military Pilot Commercial Pilot	High Performance Jet
2	Military Pilot Commercial Pilot	High Performance Jet Multiengine Jet
3	Military Pilot Airline Transport Rating	High Performance Jet Multiengine Jet
4	Military Pilot Commercial Pilot	High Performance Jet General Aviation
5	Commercial Pilot	General Aviation
6	Military Pilot Airline Transport Rating	Multiengine Jet Multiengine Prop
7	Military Pilot Commercial Pilot	High Performance Jet Multiengine Jet
8	Airline Transport Rating	Multiengine Jet Multiengine Prop

Figure 2.2 Subject Experience

subjects actively pursued flying at the time of the tests and had flown 200 or more hours in the previous year.

2.3 Pilot Evaluation of Simulation

The subject pilots were asked to evaluate the simulation. The results are displayed in Figure 2.3. Half of the pilots felt that the simulation realistically modeled the terminal approach. The remaining half felt that the simulation only had minor deficiencies which would not affect the results of experimentation.

In addition to the pilot evaluation, each subject was questioned about the cockpit displays. All pilots felt that the command window and command bugs provided all the necessary information to the pilot in a logical manner.

Workload was thought to be acceptable and in many cases quite low. This is the opinion of the subject pilots as well as the author's interpretation from personally watching each approach. The workload during the phase one testing was acceptable to low, and phase two and three were even less demanding on the pilot.

2.4 Closed Loop Speed Control Tests

The eight subject pilots were briefed on the system geometry and display information available to them. They were also told the overall objective of the testing program as well as the methods used by the timed delivery algorithm. They were then trained in the simulator until they showed a familiarity with the aircraft. The training

Responses	Evaluation
	The Aircraft Simulation:
50%	Realistically models the parameters of a terminal approach which are likely to affect the results of this experiment.
50%	Has minor deficiencies, but for the purposes of this program adequately models a terminal approach. These deficiencies should not affect the validity of test results.
0%	Has serious deficiencies which could affect the results of these tests.
0%	Is inadequate for the test program.

Figure 2.3 Pilot Evaluation of Simulation

phase took between one and eight practice terminal approaches and was dependent upon pilot instrument flying experience. At the conclusion of the training the pilots were tested.

Each pilot flew four approaches with the same wind profile and varying amounts of radar error as described in section 1.6. The four cases were each flown twice to provide additional data points for analysis. After the first four approaches the pilots were given a break. The order of the approaches was varied so that with eight subjects every combination of order was tested. These measures were taken to exclude the effects of increased learning and fatigue from the results.

The sixteen data sets from the experimentation are shown in Figure 2.4. Case zero is the no error case. Case one models the Discrete Address Beacon System and has standard deviations in range and bearing equal to 30 feet and .035 degrees. Case two has errors of 110 feet and .14 degrees. Case three models the current airport surveillance radar and has errors of 250 feet and .25 degrees.

The nominal arrival time was 486 seconds. Positive values show late arrival while negative values show early arrival. All approaches were flown successfully and the greatest arrival time error was nine seconds late. The earliest arrival was six seconds early. Of the sixty-four approaches, nine had early arrivals, forty-nine had late arrivals and six approaches were on time.

The overall average arrival time error was 1.88 seconds late. The frequency distribution of arrival time errors is plotted in Figure 2.5.

An analysis of the data is shown in Figure 2.6. The average miss

Radar Case	0	1	2	3
Subject				
1	+2	+2	+4	+1
1	+2	+1	+1	0
2	+4	+7	+8	+9
2	+1	+2	+7	+4
3	0	+3	+3	+3
3	+1	+3	+2	+5
4	0	-1	+3	+3
4	+1	0	+3	+2
5	+1	+1	+1	+5
5	-6	+3	+2	+4
6	0	+3	-1	-2
6	+2	+3	+2	+4
7	+1	-3	+2	+3
7	+1	-2	+1	+2
8	+1	-1	+2	0
8	+2	-3	-2	+8

Figure 2.4 Phase One Data

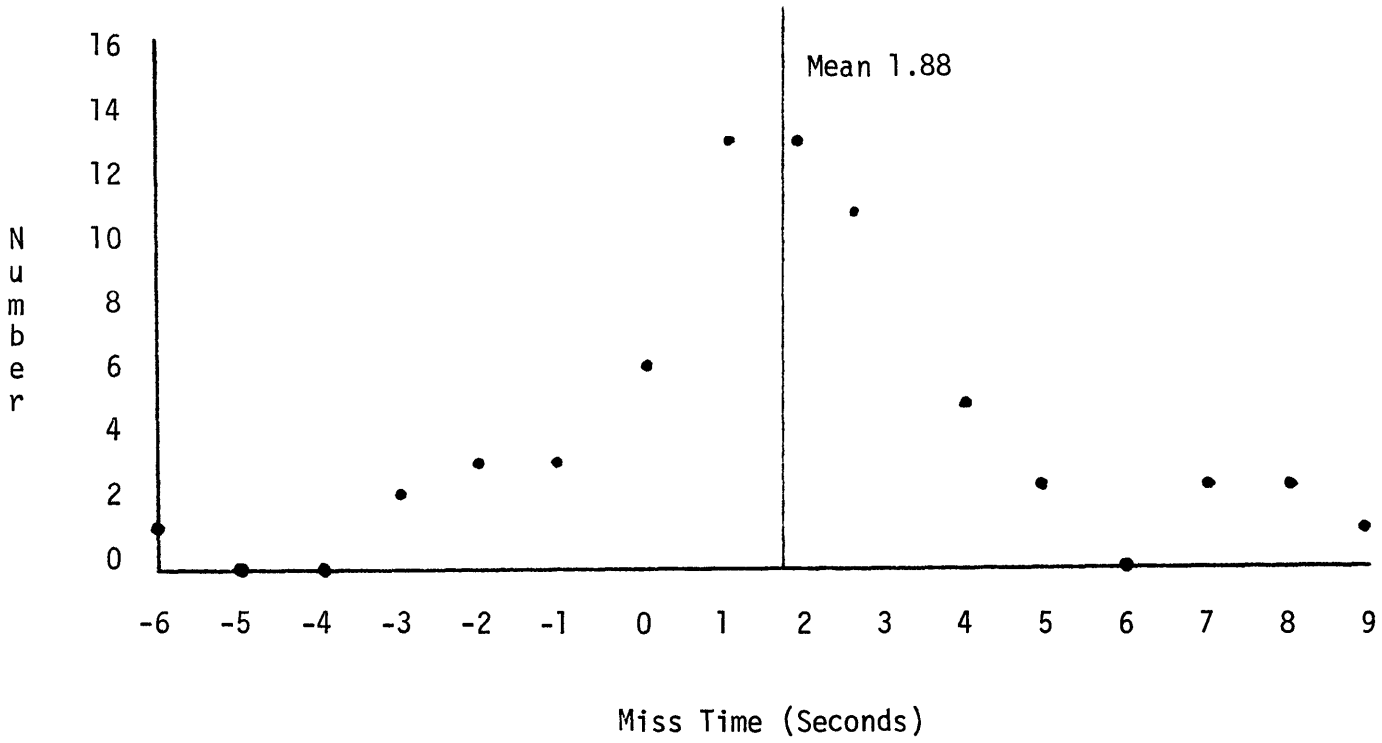

Figure 2.5 Frequency Distribution of Arrival Time Errors

Radar Case	0	1	2	3
Error Seconds	25	38	44	55
Mean	1.56	2.38	2.75	3.44
σ	1.50	1.54	1.98	2.46

Figure 2.6 Phase One Results

time without radar error was 1.56 seconds. This compares well with Morgenstern [5], who used a similar system geometry and arrived at 1.7 seconds. The average miss times for the radar error cases were 2.38, 2.75, and 3.44 seconds. No data exists for comparison.

A plot of arrival time error vs. radar error is shown in Figure 2.7. As expected, the arrival time error always increases with an increase in radar error and the function is close to linear.

2.5 Simplified Configuration

Since the arrival time errors from the phase one testing were acceptable even in the least accurate radar case, there was no need to improve the delivery algorithm. However, the question arose as to whether or not a simplified approach would yield similar results. It was decided that the closed loop speed control portion of the approach should be deleted. This was the portion of the approach where pilot workload, although still acceptable, was at it's highest point, especially with a large radar error where smoothing the commanded airspeed bug was time-consuming. It was felt that by deleting the closed loop speed control more pilot attention could be devoted to maintaining course and altitude.

The simulation was changed to allow for a constant speed final portion and four of the subject pilots were retested. Again the order was scrambled and all possible combinations were flown to eliminate the learning and fatigue factors from the results. The data for the experimentation is shown in Figure 2.8. All approaches were flown successfully

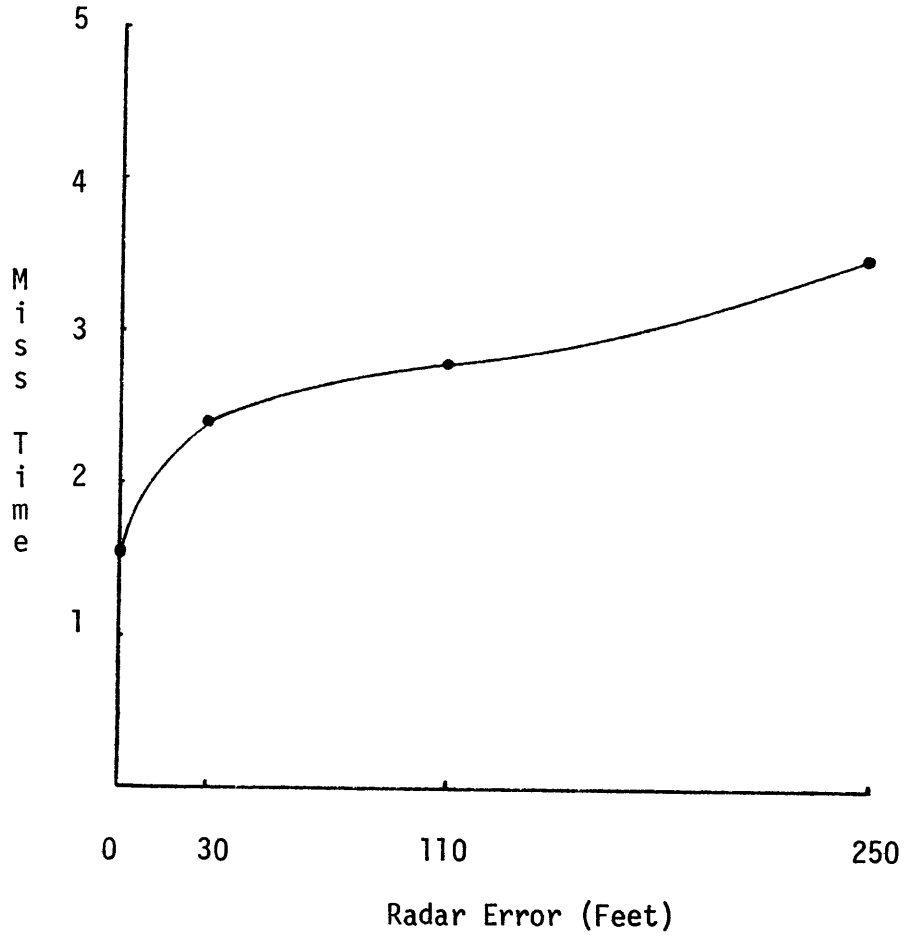

Figure 2.7 Phase One Arrival Time Error vs Radar Error

Radar Case	0	1	2	3
Subject 1	+2	-2	-2	+2
2	+2	+1	+2	-1
3	+1	+1	+2	+3
4	+1	+3	-2	+5

Figure 2.8 Phase Two Data

and the greatest arrival time error was five seconds late. The earliest arrival time was two seconds early. Of the sixteen approaches, twelve were late and four were early. All approaches had some error. The overall average arrival time error was two seconds late.

An analysis of the data is shown in Figure 2.9. The average miss time without radar error was 1.5 seconds. The average miss times for the radar error cases were 1.75, 2.0, and 2.75 seconds. The standard deviations for each of these cases was from zero to 1.48 seconds.

In order to evaulate the two phases of the testing against one another, the separated data from the phase one testing for the four pilots who flew the phase two tests is needed. The data and results for these four pilots in phase one is displayed in Figure 2.10.

A plot of the arrival time error vs. radar error is shown in Figure 2.11. As expected, the arrival time error increases with an increase in radar error and the function is close to linear. The arrival time errors for phase one and two are quite similar. It appears that the phase two system is more accurate in terms of delivery accuracy, but this may be due to increased learning on the part of the subjects. In any case, the two methods are very close in terms of accuracy and the phase two testing was considerably easier to fly.

2.6 Three Command Timed Delivery Program

Because of the results obtained in the phase two tests, the incentive to further simplify the approach was quite strong. Since the turn,

Radar Case	0	1	2	3
Error Seconds	6	7	8	11
Mean	1.5	1.75	2.0	2.75
σ	0.5	0.83	0	1.48

Figure 2.9 Phase Two Results

Radar Case	0	1	2	3
Error Seconds	13	14	19	23
Mean	1.63	1.75	2.38	2.88

Figure 2.10 Selected Phase One Results

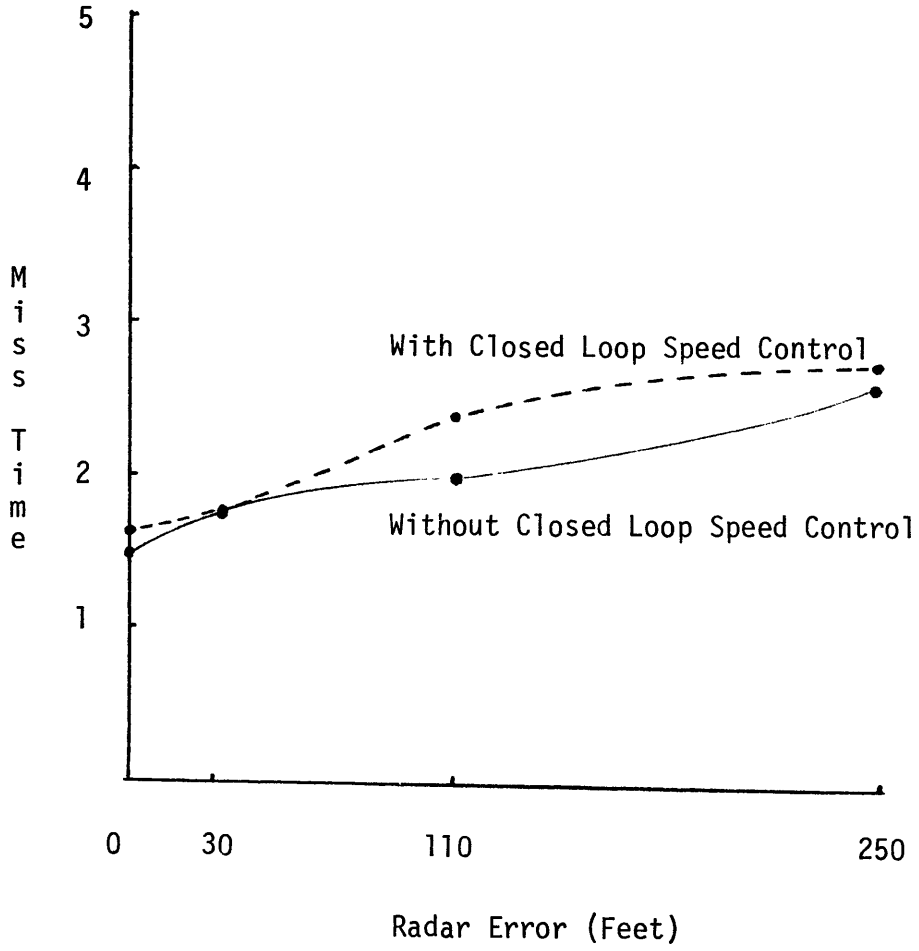

Figure 2.11 Selected Phase One and Phase Two Arrival Time Error vs Radar Error

descent, and deceleration commands were integral to the approach, the only possible simplification was to eliminate the speed command immediately following the turn. Initially, this command was designed to correct for the lateral tracking error of the radar and any deviation from a standard rate turn performed by the pilot. A greater arrival time error was expected but the increase caused by deletion of the command was not known. If path stretching was applied on the final approach, arrival errors of up to fifteen seconds could be accepted.

There were three changes implemented to accomplish this goal. The first change was the deletion of the airspeed command. Secondly, the nominal deceleration time was delayed and the interval of time for the command was increased from thirty to sixty seconds. Previously the deceleration command could only be given fifteen seconds early or late. In the phase three testing, the command could be given thirty seconds early or late. This caused a shorter time at 160 knots but this was judged to be acceptable since flight at 160 knots was called for on final approach. This increased flexibility was needed for any errors acquired between the turn and the deceleration command. Thirdly, the portion of the program which determined when to issue the deceleration command was changed slightly to bias the arrivals so that they would have a zero mean for multiple aircraft. During the phase two tests, the aircraft on the average arrived two seconds late.

With these changes, the simulation was flown twelve times by the author. Each radar error case was flown three times. The data and

analysis is displayed in Figure 2.12. All approaches were successful and the greatest arrival time error was nine seconds late. The earliest arrival time error was two seconds early. Of the twelve approaches two were early, seven were late, and three were on time.

The average miss time without radar error was one second. The miss times for the radar error cases were 1.66, 3.0, and 8.33 seconds. A plot of the arrival time error vs. radar error is shown in Figure 2.13. The arrival time error increases with an increase in radar error and the function is nearly linear.

The average miss times for cases zero, one, and two correspond favorably with earlier data. The case three miss time is considerably greater but offers no problem if path stretching is used on final approach. Here we are clearly offered a choice. We must use a better radar, implement path stretching, or maintain the airspeed command after the initial turn.

Radar Case	0	1	2	3
Run 1	0	+5	+6	+9
2	-2	0	+2	+7
3	-1	0	+1	+9
Mean	1.0	1.66	3.0	8.33

Figure 2.12 Phase Three Data and Results

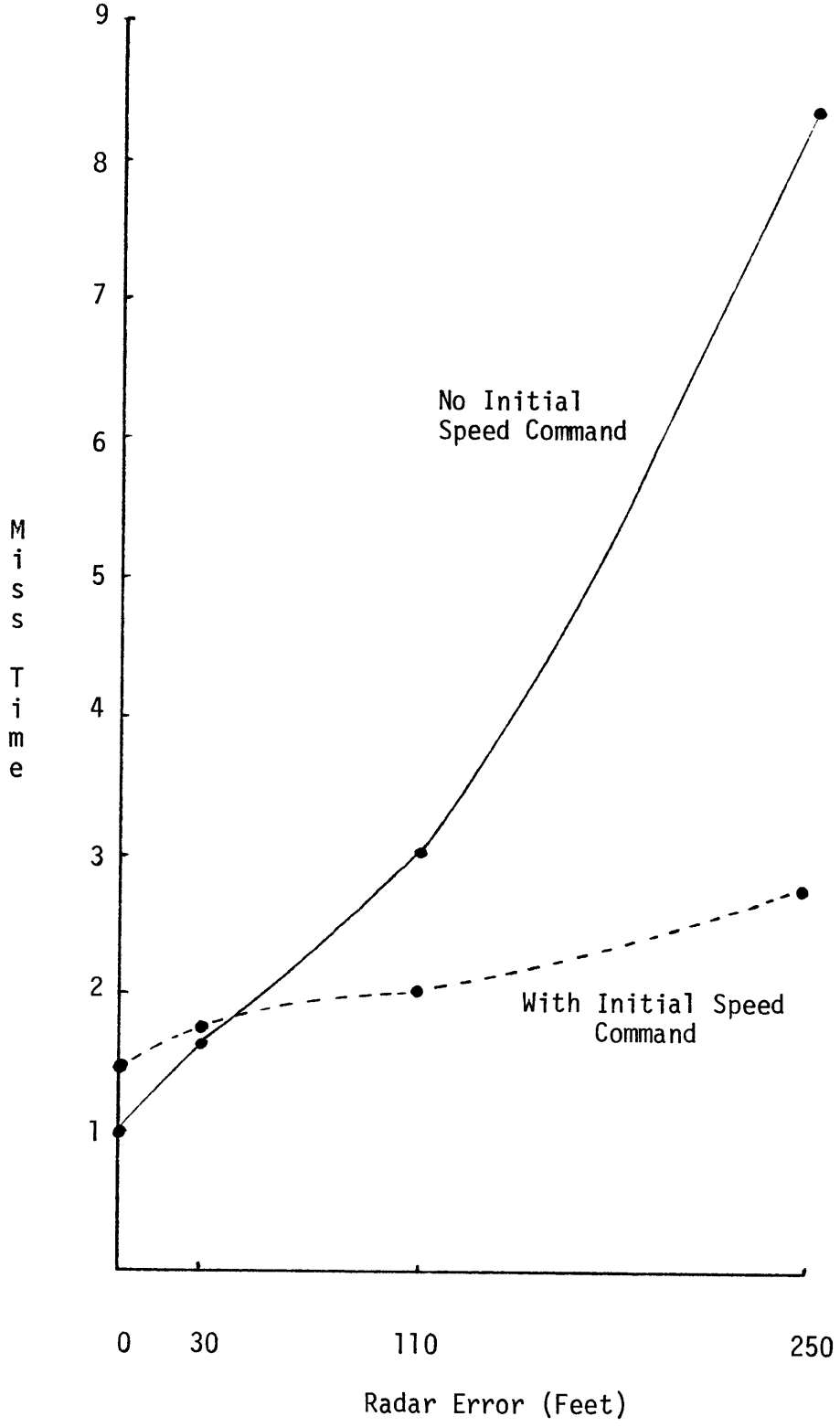

Figure 2.13 Phase Two and Three Arrival Time Error vs Radar Error

Chapter III

Conclusions and Recommendations

The results of the experimentation were very encouraging. A functional relationship between radar error and runway arrival time error was found. This relationship appears to be nearly linear and arrival time error was surprisingly small. With the use of Four-Dimensional Navigation techniques, fix to fix navigation can be performed with great accuracy, even in the terminal area. All this can be accomplished while keeping pilot workload at a low level.

Additionally, a related result was that pilot background had little effect on performance in this simulation. Although overall experience was important, as well as recent active flying, performance for pilots with multiengine aircraft flying experience was similar to those pilots which had a high performance aircraft background.

The three alternative methods for achieving delivery accuracy all performed within acceptable limits. The possible exception would be the phase three method with the case three radar. In this position, the choice is available to us to improve the radar equipment, use a slightly different method (phase two), or accept the delivery accuracy and plan on correcting for the error with optimal path stretching on final approach.

The simulation developed can be utilized in future studies in its present configuration. The entire timed delivery approach problem could be investigated with a fixed radar error. The wind could be varied to

obtain some functional relationship between wind shear and arrival time. In addition, the effect of radar placement could be investigated. In many cases, radar equipment is not located near the runway because of geographical limitations.

With minor modifications the present simulation could be used in additional studies. One recommendation would be to implement a constant speed optimal path stretching routine from the final approach fix to the runway. Finally, since the previous simulations all displayed the command information to the pilot, the effect of completely manual operation could be investigated. This could be done by eliminating the command information from the cockpit and adding an air traffic controller who would receive the command information from the computer and transmit the information to the pilot. This would provide information on the value of retro-fitting aircraft with the necessary equipment to display a command window and command bugs.

References

1. Malherbe, G. "Modeling of Wind and Radar for Simulation in Four-Dimension Navigation Environment," Flight Transportation Laboratory Report R76-8, M.I.T., September 1976.

2. Ley, B.G. Computer Aided Analysis and Design for Electrical Engineers, Holt, Reinhart and Winston, Inc., New York, 1970, pp. 561-599.

3. Report of Department of Transportation Air Traffic Control Advisory Committee, Volume 2, December 1969.

4. Hsin, C.C. "An Analytical Study of Advanced Terminal Area Air Traffic Management and Control," Flight Transportation Laboratory Report R77-1, M.I.T., 1977.

5. Morgenstern, B. "Evaluation of the Airborne Traffic Situation Display as a Backup Terminal ATC Device," S.M. Thesis, Department of Aeronautics and Astronautics, M.I.T., 1974.